Available online at www.sciencedirect.com

SCIENCE DIRECT®

Marine Micropaleontology 58 (2006) 243–258

MARINE MICROPALEONTOLOGY

www.elsevier.com/locate/marmicro

# The influence of seawater carbonate ion concentration $[CO_3^{2-}]$ on the stable carbon isotope composition of the planktic foraminifera species *Globorotalia inflata*

Iris Wilke [a,*], Torsten Bickert [a], Frank J.C. Peeters [b]

[a] *Fachbereich Geowissenschaften, Universität Bremen, Postfach 330 440, Klagenfurter Straße, 28359 Bremen, Germany*
[b] *Faculty of Earth and Life Sciences (FALW), Vrije Universiteit, De Boelelaan 1085, 1081 HV Amsterdam, The Netherlands*

Received 24 November 2005; accepted 25 November 2005

## Abstract

We sampled the upper water column for living planktic foraminifera along the SW-African continental margin. The species *Globorotalia inflata* strongly dominates the foraminiferal assemblages with an overall relative abundance of 70–90%. The shell $\delta^{18}O$ and $\delta^{13}C$ values of *G. inflata* were measured and compared to the predicted oxygen isotope equilibrium values ($\delta^{18}O_{eq}$) and to the carbon isotope composition of the total dissolved inorganic carbon ($\delta^{13}C_{DIC}$) of seawater. The $\delta^{18}O$ of *G. inflata* reflects the general gradient observed in the predicted $\delta^{18}O_{eq}$ profile, while the $\delta^{13}C$ of *G. inflata* shows almost no variation with depth and the reflection of the $\delta^{13}C_{DIC}$ in the foraminiferal shell seems to be covered by other effects. We found that offsets between $\delta^{18}O_{shell}$ and predicted $\delta^{18}O_{eq}$ in the surface mixed layer do not correlate to changes in seawater $[CO_3^{2-}]$.

To calculate an isotopic mass balance of depth integrated growth, we used the oxygen isotope composition of *G. inflata* to estimate the fraction of the total shell mass that is grown within each plankton tow depth interval of the upper 500 m of the water column. This approach allows us to calculate the $\Delta\delta^{13}C_{interval\ added\text{-}DIC}$; i.e. the isotopic composition of calcite that was grown within a given depth interval. Our results consistently show that the $\Delta\delta^{13}C_{IA\text{-}DIC}$ correlates negatively with in situ measured $[CO_3^{2-}]$ of the ambient water. Using this approach, we found $\Delta\delta^{13}C_{IA\text{-}DIC}/[CO_3^{2-}]$ slopes for *G. inflata* in the large size fraction (250–355 μm) of $-0.013‰$ to $0.015‰$ $(\mu mol\ kg^{-1})^{-1}$ and of $-0.013‰$ to $0.017‰$ $(\mu mol\ kg^{-1})^{-1}$ for the smaller specimens (150–250 μm). These slopes are in the range of those found for other non-symbiotic species, such as *Globigerina bulloides*, from laboratory culture experiments. Since the $\Delta\delta^{13}C_{IA\text{-}DIC}/[CO_3^{2-}]$ slopes from our field data are nearly identical to the slopes established from laboratory culture experiments we assume that the influence of other effects, such as temperature, are negligibly small. If we correct the $\delta^{13}C$ values of *G. inflata* for a carbonate ion effect, the $\delta^{13}C_{shell}$ and $\delta^{13}C_{DIC}$ are correlated with an average offset of 2.11.

*Keywords:* Planktic foraminifera; Stable isotopes; Carbonate ion effect; *Globorotalia inflata*; Cape Basin

## 1. Introduction

Planktic foraminifera usually use the dissolved inorganic carbon (DIC) of the surrounding seawater to build their calcitic shells. Hence, they may be an excellent tool for the reconstruction of the $\delta^{13}C_{DIC}$ of past ocean waters, assuming equilibrium fractionation during cal-

---

* Corresponding author. Tel.: +49 421 218 3974; fax: +49 421 218 4451.

*E-mail address:* iwilke@uni-bremen.de (I. Wilke).

0377-8398/$ - see front matter © 2005 Elsevier B.V. All rights reserved.
doi:10.1016/j.marmicro.2005.11.005

cification. Once this requirement is fulfilled or disequilibrium effects have been quantified, $\delta^{13}C_{DIC}$ can be used as a proxy for past oceanic circulation and variations of the carbonate system, biological productivity and nutrient cycling in surface waters (Kahn and Williams, 1981; Broecker and Peng, 1982; Bouvier-Soumagnac and Duplessy, 1985; Kroon and Ganssen, 1989). The $\delta^{13}C_{DIC}$ of the ambient seawater is mainly controlled by a kinetic fractionation during the photosynthesis–respiration cycle, and by a thermodynamic fractionation during the exchange of $CO_2$ between the atmosphere and the ocean (Broecker and Maier-Reimer, 1992; Charles et al., 1993; Lynch-Stieglitz et al., 1995).

Previous studies have shown that the $\delta^{13}C$ of planktic foraminifera calcite often deviates from the $\delta^{13}C_{DIC}$. Ontogenetic and metabolic effects, kinetic fractionation effects and the effect of photosynthetic utilization by symbionts have been discussed (e.g. Shackleton and Vincent, 1978; Wefer and Berger, 1991; Ravelo and Fairbanks, 1995; Spero and Lea, 1996; Mulitza et al., 1999; Peeters et al., 2002). Furthermore, the carbonate ion concentration $[CO_3^{2-}]$ of seawater appears to be a major feature influencing the $\delta^{13}C$ of the shell carbonate (Spero et al., 1997; Bijma et al., 1998). These authors demonstrated that the $\delta^{13}C$ of planktic foraminifera decreases with increasing $[CO_3^{2-}]$ of the culture medium, possibly due to a combination of kinetic and metabolic isotope effects (Spero et al., 1997; Zeebe et al., 1999).

Since ice core records indicate lower atmospheric $CO_2$ concentrations during glacial times (Jouzel et al., 1993; Petit et al., 1999), different hypotheses arose to explain this lower atmospheric $CO_2$ content. Archer and Maier-Reimer (1994) put forward the hypothesis of an increased ocean alkalinity, i.e. a higher $[CO_3^{2-}]$ during glacial times. This was also suggested by Sanyal et al. (1995) using boron isotopes ($\delta^{11}B$) measurements for seawater pH reconstructions. An elevated seawater pH during glacial times might explain the more negative $\delta^{13}C$ values of planktic foraminifera calcite found in glacial sediments without altering mean ocean $\delta^{13}C_{DIC}$ (Lea et al., 1999).

This paper is a contribution to the field investigations of the carbonate ion effect on the $\delta^{13}C$ of planktic

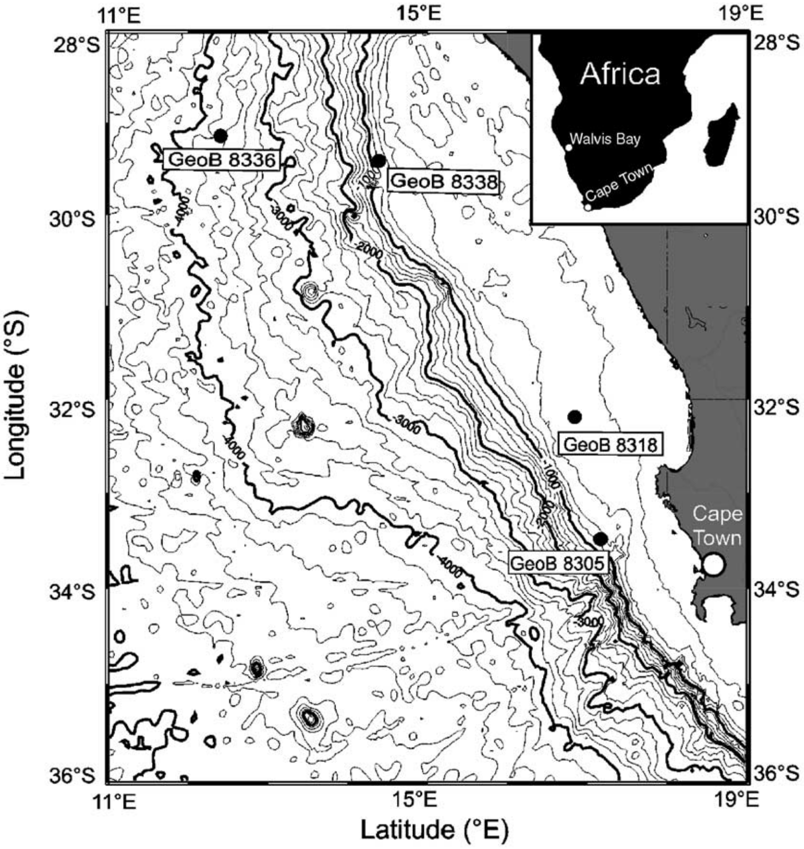

Fig. 1. Map of the study area in the eastern South Atlantic (Cape Basin). Closed circles indicate location of plankton tow casts taken during M57/1 in January/February 2003: GeoB8336, 8338, 8318 and 8305. Inset shows an overview map of the southern African continent.

Table 1
Station location and general hydrographic information

| GeoB station | Date | Longitude (E) | Latitude (S) | Water depth (m) | SST (°C)[a] | MLD (m)[b] |
|---|---|---|---|---|---|---|
| 8305 | 23.01.03 | 17°10.17 | 33°28.55 | 712 | 21.10 | 47 |
| 8318 | 28.01.03 | 16°48.47 | 32°09.16 | 307 | 18.05 | 12 |
| 8336 | 02.02.03 | 12°20.14 | 29°12.14 | 3626 | 21.00 | 37 |
| 8338 | 03.02.03 | 14°19.42 | 29°29.94 | 915 | 20.67 | 21 |

[a] SST = sea surface temperature.

[b] MLD = mixed layer depth. The depth of the mixed layer is defined at that depth at which the water temperature is 0.5 °C less than the SST.

foraminifera. Under natural conditions this topic has been discussed for the following species: *Globigerina bulloides* and *Globigerinoides ruber* (Russell and Spero, 2000; Peeters et al., 2002), *Globorotalia scitula* (Itou et al., 2001), *P. obliquiloculata* (Russell and Spero, 2000) and *Neogloboquadrina pachyderma* (sin.) (Bauch et al., 2002). Here the non-symbiotic deep-dwelling species *Globorotalia inflata* were chosen, sampled by stratified plankton tows at four stations in the southeast Atlantic Ocean (Fig. 1, Table 1).

## 2. Material and analysis

Plankton tow samples and samples of the ambient seawater investigated in this study were collected during Meteor cruise M57/1 in January/February 2003 in the southeastern Atlantic Ocean (Cape Basin) (Fig. 1) (Schneider et al., 2003). Planktic foraminifera were collected with a Multiple Opening–Closing Net (multinet). The nets of 63 μm mesh size were towed vertically with maximum winch speed of 0.5 m $s^{-1}$ at 20 m depth intervals for a shallow (0–20, 20–40, 40–60, 60–80 and 80–100 m) and a deep cast (100–200, 200–300 and 300–500 m). On board all samples were conserved with a saturated $HgCl_2$ solution and stored at 4 °C. Planktic foraminifera species were picked out from the wet sample. All specimens in the size fraction >150 μm were counted and identified using the taxonomy of Bé et al. (1977) and Hemleben et al. (1989).

Stable isotope determinations of *G. inflata* in two size classes (150–250 μm and 250–355 μm) were conducted at the University of Bremen using a Finnigan Mat 252 mass spectrometer equipped with an automatic carbonate preparation device. Isotope composition is given in the usual $\delta$-notation and is calibrated to Vienna Pee Dee Belemnite (V-PDB) standard. The precision of the measurements at $1\sigma$ based on replicates of an internal standard (Solnhofen limestone) was ±0.05‰.

Water samples were collected shortly before the plankton sampling procedure using a Rosette equipped with 18 water samplers (each 10 l volume). Each station was accompanied by a CTD cast providing information on the vertical structure of the water column including temperature, salinity and fluorescence. Water from each sampler was filled into glass bottles, carefully avoiding air bubbles in the filling tube and in the bottle to minimize the exchange of $CO_2$ between water and air. Samples for $\delta^{13}C$ of the total dissolved inorganic carbon (DIC) were conserved with a saturated $HgCl_2$ solution and the bottles were sealed airtight with molten paraffin. The DIC was extracted from seawater by adding 100% $H_3PO_4$ at 25 °C, and measured on Gas Bench II system (Finnigan MAT), equipped with a fully automated extraction line. The $\delta^{13}C$ of $\sum CO_2$ was measured with a Finnigan MAT Delta Plus mass spectrometer directly coupled to the Gas Bench via an open split. All $\delta^{13}C$ measurements were run triplicate. The external reproducibility of the measurements at $1\sigma$ was better than ±0.06‰.

In this study, we calculated the $\delta^{18}O$ of the seawater by using the linear relationship between salinity and $\delta^{18}O_w$ established for Southern Ocean by Duplessy et al. (1991):

$$\delta^{18}O_w\ (‰, PDB) = -18.791 + 0.546 * S \tag{1}$$

where $S$ denoted the salinity. The oxygen "equilibrium calcite values", $\delta^{18}O_{eq}$, are calculated using the calculated oxygen isotope composition of seawater ($\delta^{18}O_w$) and in situ temperature ($T$). We use the equation of Kim and O'Neil (1997) that is based on their inorganic calcite precipitation experiment. The oxygen isotope equilibrium for inorganic (synthetic) calcium carbonate precipitated at low temperatures (10–40 °C) follows the relationship:

$$\delta^{18}O_{eq} = 25.778 - 3.333 * (43.704 + T)^{0.5} + \delta^{18}O_w \tag{2}$$

Water samples for Total Alkalinity (TA) and total dissolved inorganic carbon (DIC) were filtered onboard and treated similar as the samples for $\delta^{13}C$. TA and DIC measurements were conducted at the Alfred-Wegener Institute for Polar and Marine Research in Bremerhaven, Germany by titration and continuous flow analysis (Stoll et al., 2001), respectively. The external reproducibility of the measurements at $1\sigma$ was ±4.32 $\mu mol \cdot kg^{-1}$ and ±1.86 $\mu mol \cdot kg^{-1}$ for TA and DIC, respectively.

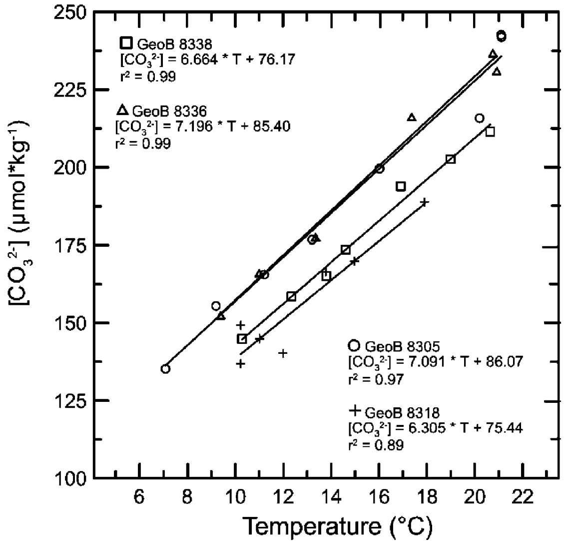

Fig. 2. Seawater temperature versus carbonate ion concentration ($[CO_3^{2-}]$) of the upper 500 m of the water column at stations GeoB8336, 8338, 8318 and 8305.

The carbonate ion concentration $[CO_3^{2-}]$ were calculated from DIC and TA using the software program CO2SYS (version 5.1) of Lewis and Wallace (1998). We used the constants of Weiss (1974) for $k_o$ (the solubility of $CO_2$ in seawater), Roy et al. (1993) for $k_1$ (2s = 2%) and $k_2$ (2s = 1.5%), the equilibrium constants that define the speciation of $CO_2$ in seawater, and Dickson (1990) for $k_B$ (dissociation constant of borate). The effects of pressure on $k_1$ and $k_2$ are from Millero (1995) and on $k_B$ from Millero (1979).

Since temperature and $[CO_3^{2-}]$ are well correlated at each station (Fig. 2), we used a linear regression between the two parameters to estimate $[CO_3^{2-}]$ for depths where we have no measurements in order to obtain a continuous profile of $[CO_3^{2-}]$ with depth.

## 3. Hydrography of the Cape Basin

The Benguela Current Upwelling region is one of the four major eastern ocean boundary currents of the world. Although upwelling occurs all along the African west coast, several regions of recurring patches of intense upwelling have been identified. The largest and most persistent cell is the Lüderitz upwelling cell, which effectively divides the Benguela upwelling system into a northern and southern regime. The upwelling cells are generally located in regions where there is a change in orientation of the coastline (Shannon and Nelson, 1996). In general, the wind dominated upwelling system brings cold nutrient-rich water to the surface.

Fig. 3 shows temperature–salinity plots for stations GeoB8336 (~3000 m water depth, open ocean) and GeoB8318 (307 m water depth, shelf). Based on temperature and salinity characteristics four water masses could be identified (Shannon, 1985; Valentine et al., 1993; Gordon, 1996): South Atlantic Surface Water (SASW), South Atlantic Central Water (SACW), Antarctic Intermediate Water (AAIW) and North Atlantic Deep Water (NADW). Table 2 lists the physical characteristics of each water mass and the depth at which it was identified at each site. It is the SACW water that upwells along the coast between 18°S and 34°S. This water mass is found throughout the SE Atlantic between surface waters and Antarctic Intermediate (AAIW) waters or it extends to the bottom on the continental shelf. It is formed at the Subtropical Con-

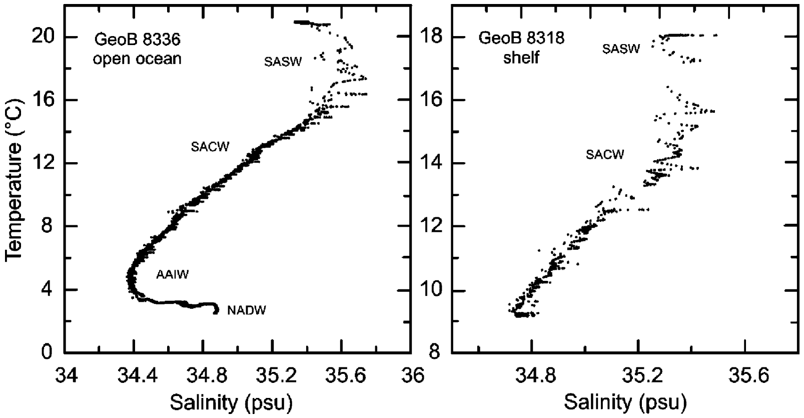

Fig. 3. Temperature–salinity plot for stations GeoB8336 (~3000 m, open ocean) and 8318 (~250 m, shelf). In total four different water masses could be identified: South Atlantic Surface Water (SASW), South Atlantic Central Water (SACW), Antarctic Intermediate Water (AAIW) and North Atlantic Deep Water (NADW). For further information see Table 2.

Table 2
Physical characteristics of water masses encountered at CTD station GeoB8336

| Water mass | Temp. range (°C) | Salinity range (psu) | Depth range (m) | Density (sigma-*t*) |
|---|---|---|---|---|
| SASW | 15.5–21.3 | 35.3–35.7 | 0–60 | 25.0–26.0 |
| SACW | 6.1–15.2 | 34.4–35.4 | 60–600 | 26.3–27.3 |
| AAIW | 4.0–6.0 | 34.3–34.5 | 780 (core) | 27.3–27.5 |
| NADW | <3.0 | >34.5 | 1100 (core) | 27.8–28.0 |

vergence (STC) by sinking and northward spreading of mixed subtropical and subantarctic water masses. Its characteristic temperature and salinity ranges between 6.1 °C–15.2 °C and 34.4–35.4 psu, respectively. At stations GeoB8318 and GeoB8338, the influence of upwelling waters is reflected by a shallow mixed layer and a shallower chlorophyll maximum (Fig. 4), compared to sites located more off-shore. It has been shown before that upwelling may significantly change the water carbonate chemistry of surface waters (Peeters and Brummer, 2002). Our measurements show that the difference in the carbonate ion concentration at upwelling station GeoB 8318 is ~60 μmol kg$^{-1}$ lower compared to GeoB 8305 (242.0 μmol kg$^{-1}$) (Table 3), which is located outside the upwelling region.

## 4. Results

### 4.1. Planktic foraminifera abundance

The species *G. inflata* strongly dominates the faunal assemblage at all stations with an overall relative abundance of 70–90%. The absolute abundance of *G. inflata* (ind. m$^{-3}$) individuals >150 μm in the upper 500 m (at station GeoB8318 in the upper 300 m) is highest at station GeoB8338 with ~450 ind m$^{-3}$ and lowest on the shelf at GeoB8318, where only ~50 ind. m$^{-3}$ occur (Fig. 4). Maxima in the shell concentration of *G. inflata* are found within the mixed layer and the thermocline, coincident to highest chlorophyll-a values However, it is worth mentioned that chlorophyll-a is not likely to be an accurate predictor of true food availability. In general, the shell concentration decreases with depth in the water column.

Besides *G. inflata*, the deep dwelling species *G. scitula* were abundant in relatively high concentrations below 100 m water depth, thus below the thermocline. The nearcoast station GeoB8338 (915 m) shows elevated numbers of *G. bulloides*, a species known to occur also in nutrient-rich upwelling waters (Thiede, 1975; Prell and Curry, 1981). At GeoB8318, located on the shelf, we found increased numbers of the cold water

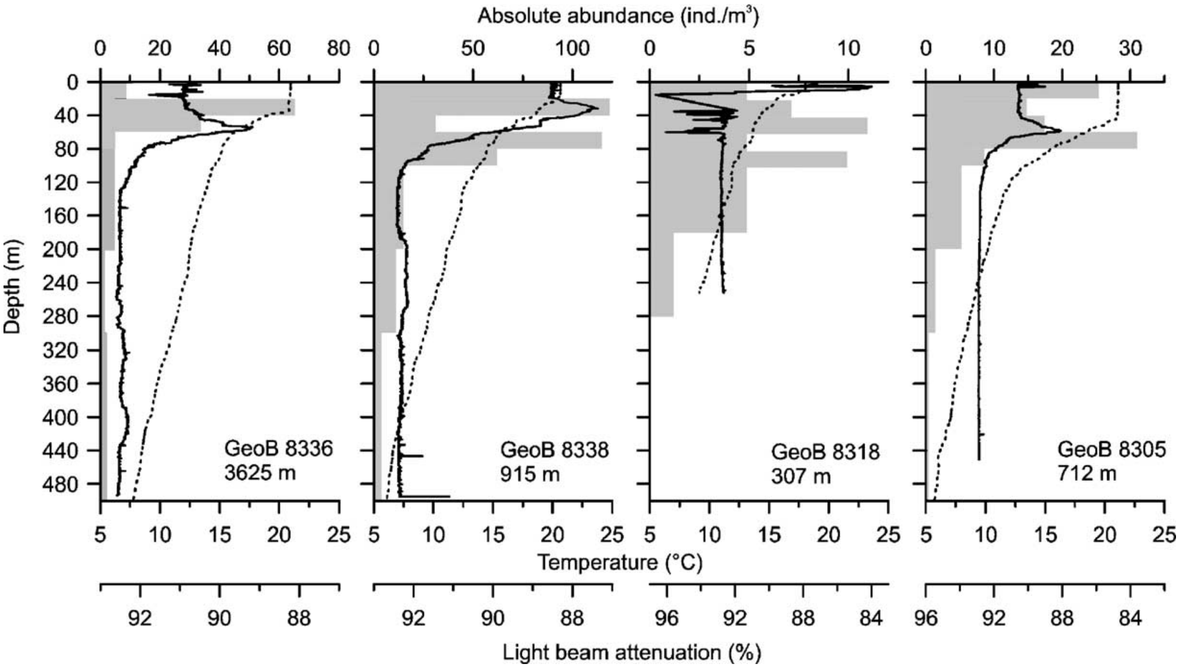

Fig. 4. Graphs showing hydrographic conditions (temperature, light beam attenuation) and absolute abundances (ind./m$^3$) of *G. inflata* (>150 μm) as standing stock in the upper water column at stations GeoB8336, 8338, 8318 and 8305 collected in seven depth intervals. The widths of the gray bars cover the depth range of each sampling interval. Note different scales.

species *N. pachyderma* (sin). In contrast, the southern most station (GeoB8305) is characterized by increased numbers of tropical and subtropical species such as *Orbulina universa*, *G. ruber* white and *Globorotalia menardii*, likely indicating warm Indian Ocean water that enter the South Atlantic Ocean via Agulhas leakage (Peeters et al., 2004).

### 4.2. Stable isotopes

#### 4.2.1. Oxygen

The vertical profiles of calculated $\delta^{18}$O equilibrium calcite ($\delta^{18}O_{eq}$) (according to Kim and O'Neil, 1997) show a strong increase with depth in the water column (Fig. 5). This is largely due to the observed decreasing temperature trend. The oxygen isotope composition of *G. inflata* ($\delta^{18}O_{inflata}$) also shows an increase with depth reflecting the general gradient of the $\delta^{18}O_{eq}$ profiles. In the mixed layer the $\delta^{18}$O of *G. inflata* (250–355 μm) is close to the $\delta^{18}O_{eq}$ values with an average offset of +0.05‰; except for station GeoB8318 where the values are lower by −0.22‰. Below the mixed layer, the $\delta^{18}$O values are generally lower than the equilibrium values by about 0.5‰ to 1.1‰ (Table 4).

#### 4.2.2. Carbon

At the investigated stations, the $\delta^{13}C_{DIC}$ is highest in the surface mixed layer, and generally shows a sharp decrease below the mixed layer (Fig. 5). Minimum $\delta^{13}C_{DIC}$ values occur at approximately 100 m and remain nearly constant below this depth. The carbon isotope values of *G. inflata* do not reflect the sharp decrease with depth observed in the $\delta^{13}C_{DIC}$. While showing some scatter in the upper mixed layer, *G. inflata* shows a slight increase to heavier $\delta^{13}$C values with depth. The $\delta^{13}$C of *G. inflata* ranges between +0.15‰ and +0.76‰ in the 150–250 μm size class, and between +0.45‰ and +0.88‰ in the larger size fraction (250–355 μm). In contrast to $\delta^{18}$O values, the $\delta^{13}$C values of *G. inflata* show a clear size dependence. Smaller individuals are on average 0.23‰ ± 0.11‰ ($1\sigma$; $n=20$) lighter compared to the individuals of the larger size fraction (Fig. 5, Table 4).

Specimens of *G. inflata* in the 250–355 μm size fraction are on average 0.50‰ lighter than the $\delta^{13}C_{DIC}$ regarding the upper 500 m of the water column. Smaller specimens (150–250 μm) show an average offset of −0.87‰. In the upper most depth interval (0–20 m) the deviations from $\delta^{13}C_{DIC}$ were usually highest: −1.00‰ for specimens in the larger size fraction and −1.39‰ for the smaller specimens.

## 5. Discussion

### 5.1. Habitat depth and integrated calcification

*G. inflata* is known to be a species inhabiting transitional to subpolar oceanic regions (Bé and Hutson, 1977; Hemleben et al., 1989). We found maximum concentrations of *G. inflata* within the thermocline, which is in agreement with observations by Fairbanks et al. (1982). Along the SW-African continental margin this corresponds to an average depth of 20–80 m depending on the depth of the thermocline. Since the oxygen isotopic composition of *G. inflata* increases with increasing depth in the water column, it is evident that continued shell growth occurs over depth, and is not restricted to a fixed or constant depth level. Specimens that are caught below the surface mixed layer are lighter than the in situ expected equilibrium, indicating that a fraction of the shell was grown at shallower depths. To quantify the amount of calcite precipitated within a given depth interval, we use an oxygen isotope mass balance model that is explained in more detail in the appendix. This model allows to quantify the amount of calcite precipitated within each depth interval, assuming shell growth starts at the sea surface.

Fig. 6 shows the fraction of the total shell mass that is grown for each plankton depth interval as calculated from the measured $\delta^{18}$O shell value in the upper 500 m of the water column. At stations GeoB8338 and GeoB8336, *G. inflata* builds high amounts of its calcite in the surface mixed layer (~15–20%). In contrast, at the southernmost station GeoB8305, *G. inflata* precipitates high amounts within the thermocline. At GeoB8318 on the shelf the maximum of calcification occurs in ~100 m water depth. Our observations indicate that *G. inflata* does not have a uniform shell mass development as a function of depth, but that depth integrated calcification is controlled by the local hydrography.

In this study we sampled the upper 500 m of the water column. The $\delta^{18}$O shell profiles of stations of 8338 and 8336 show that the oxygen isotope composition of *G. inflata* in the 200–300 m plankton tow is the same as in the 300–500 m plankton tow, indicating that shell growth likely ceased in the upper 500 m. For station 8305 the value in the deepest net is clearly higher compared to the value in the 200–300 m plankton tow. Obviously deeper plankton tows would have been needed to investigate if shell growth continued below 500 m. At station 8318 observations go as deep as 300 m. Here the $\delta^{18}$O values of the 150–200 m and 200–300 m tow interval are alike,

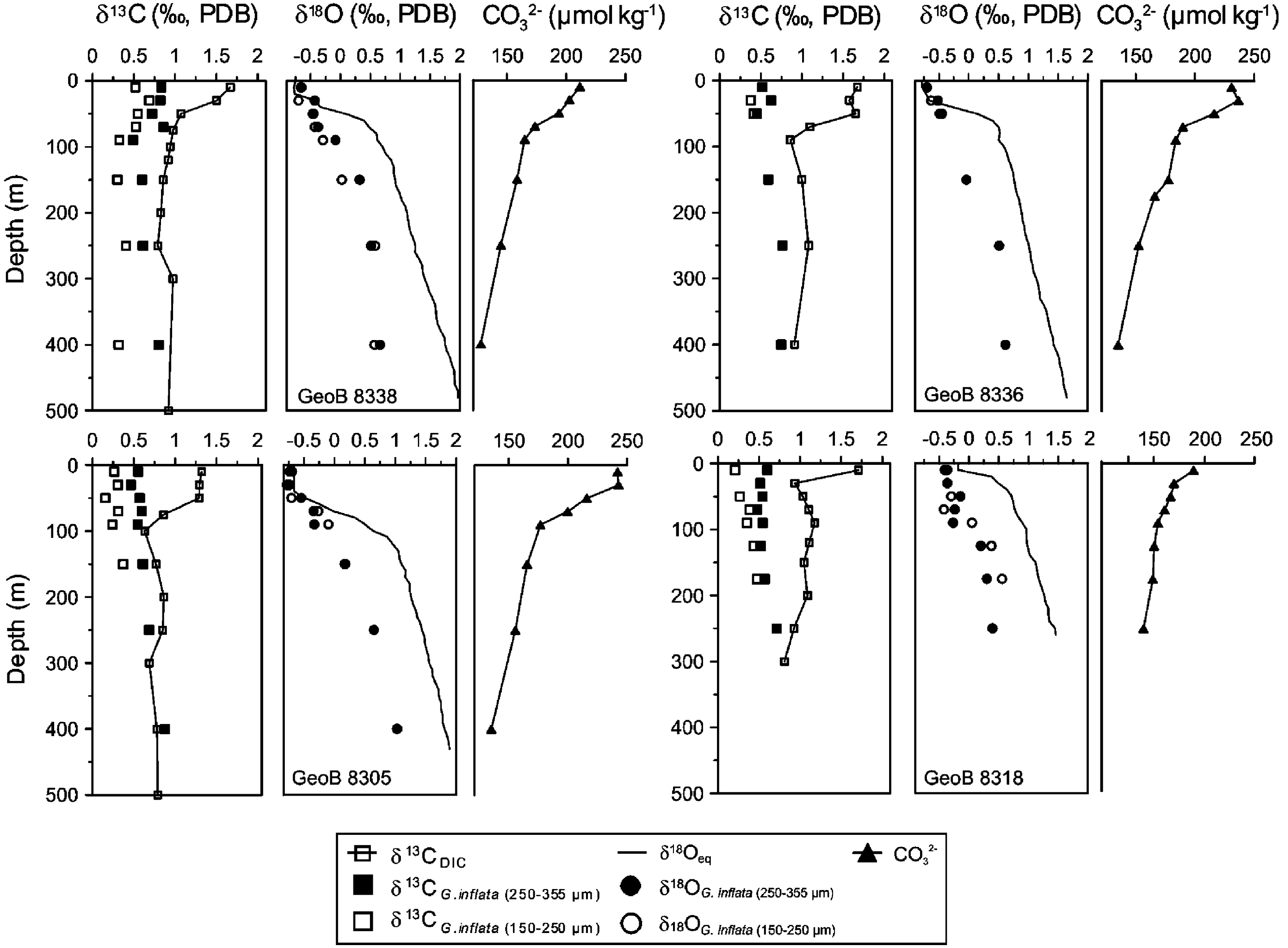

Fig. 5. The $\delta^{18}$O and $\delta^{13}$C composition of *G. inflata* (150–250 (open dots/open squares) and 250–355 μm (filled dots/filled squares)) in the upper water column in the Cape Basin. The foraminiferal $\delta^{18}$O values are directly compared to equilibrium values ($\delta^{18}O_{eq}$), while the foraminiferal $\delta^{13}$C values are directly compared to in situ $\delta^{13}C_{DIC}$ values. For each station the [$CO_3^{2-}$] profile in the water column is shown.

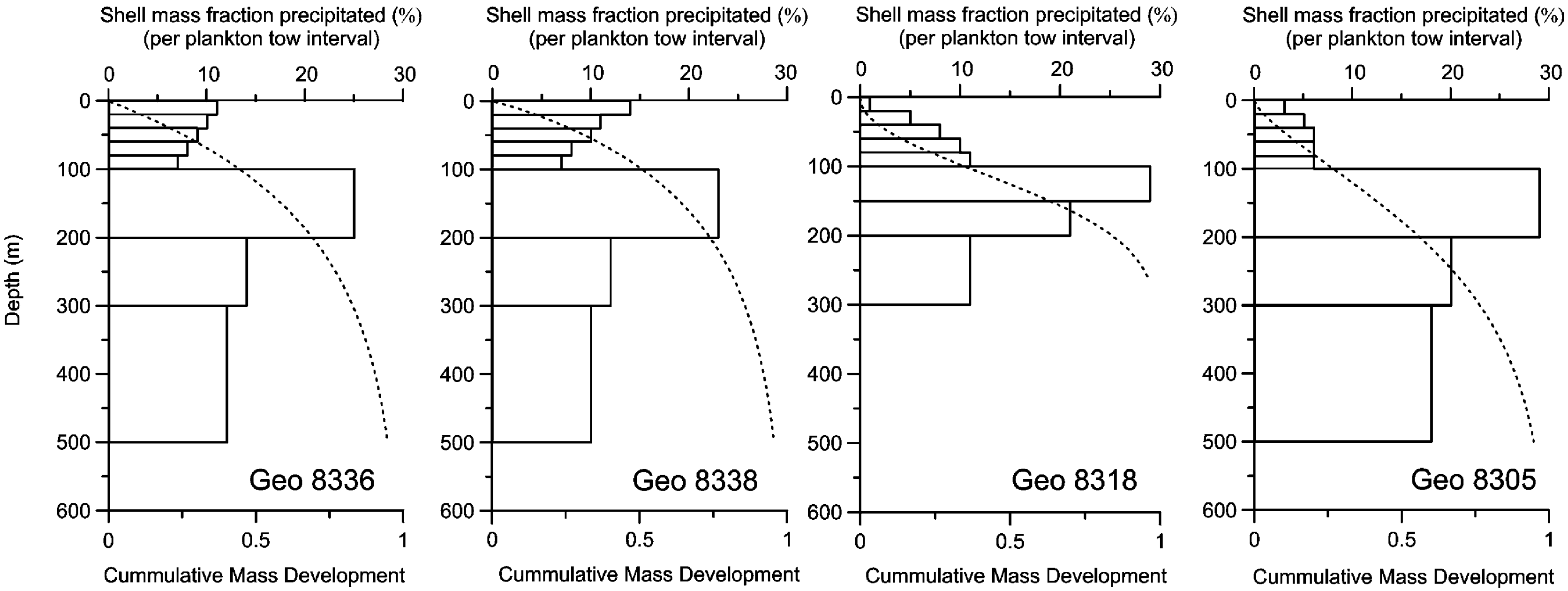

Fig. 6. Bars showing the shell mass fraction precipitated (%) by *G. inflata* in the depth intervals in the upper 500 m of the water column. The dashed line shows the cumulative mass development, which gives us for example information about the depth where shell growth ceases.

suggesting that shell growth may have stopped already in the upper 200 m.

In the following we will make use of the information on the depth-integrated calcification within the upper water column to unravel the potential influence of $[CO_3^{2-}]$ on the $\delta^{13}C_{shell}$ of *G. inflata*.

### 5.2. The influence of $[CO_3^{2-}]$ on $\delta^{18}O_{inflata}$?

Besides temperature and the isotopic composition of seawater, the $\delta^{18}O$ of planktic foraminiferal calcite may be affected by the carbonate chemistry of the ambient seawater (Spero et al., 1997). These authors have shown that the $\delta^{18}O$ composition of the species *G. bulloides* changes with a slope of $-0.005‰ \cdot (\mu mol \cdot kg^{-1})^{-1}$. As the $[CO_3^{2-}]$ in the upper water column at our field stations ranges from 188 to 242 $\mu mol \cdot kg^{-1}$, this could affect the oxygen isotope composition of the foraminiferal shell by 0.27‰, using the slope of Spero et al. (1997).

In this study we use the equation of Kim and O'Neil (1997) to calculate the expected values for equilibrium calcite ($\delta^{18}O_{eq}$). We here assume that specimens collected within the surface mixed layer have precipitated all their calcite under the constant environmental conditions of the surface mixed layer. As such, the $\delta^{18}O$ composition of these specimens should be identical to the expected mixed layer equilibrium value. If not, the difference between $\delta^{18}O_{shell}$ minus $\delta^{18}O_{eq}$ (to correct for the temperature effect) might be related to the $[CO_3^{2-}]$. Our mixed layer observations include seven data points for which the offset from shell equilibrium has been plotted versus the in situ $[CO_3^{2-}]$ of the mixed layer (graph not shown). The correlation coefficient ($r$) is 0.37, which indicates that there is no firm basis to conclude that there is a relation between the oxygen isotope composition of the shell and the $[CO_3^{2-}]$ of the ambient water at both $\alpha = 0.01$ and $\alpha = 0.05$ confidence levels (for the correlation coefficient a student $t$-value of 0.90 was found). Since our data indicate that the correlation coefficient is not statistically different from zero, the use of the slope obtained during this procedure is meaningless. It has also been shown by King and Howard (2005) that the offsets from $\delta^{18}O_{eq}$ for *G. bulloides* do not correlate to changes in seawater $[CO_3^{2-}]$, which contradicts findings obtained from laboratory experiments (Spero et al., 1997).

We therefore conclude that: (1) there is no significant relationship between the oxygen isotope composition of the shell and the $[CO_3^{2-}]$ of the ambient seawater, and (2) that the average difference between the $\delta^{18}O_{eq}$ and the in situ equilibrium values, based on the equation of Kim and O'Neil (1997), for the specimens collected within the mixed layer is $-0.01‰$. Consequently, the equation of Kim and O'Neil is well suited, at least for our stations in the Southeast Atlantic Ocean, to predict the oxygen isotope composition of *G. inflata*.

### 5.3. $\delta^{13}C_{inflata}$ and $\delta^{13}C_{DIC}$

The $\delta^{13}C_{DIC}$ is usually enriched within the photic zone because of the preferential consumption of the lighter isotope $^{12}C$ during photosynthesis, while in deeper waters $\delta^{13}C_{DIC}$ is depleted due to the remineralisation of organic matter (Broecker and Peng, 1982). It has been suggested that the $\delta^{13}C$ of a foraminiferal shell is a function of the $\delta^{13}C_{DIC}$ (Spero, 1992). Consequently, one would expect that the decreasing $\delta^{13}C_{DIC}$ with depth in the water column is reflected in the $\delta^{13}C$ of *G. inflata*. Our results indicate that this apparently is not the case: the $\delta^{13}C$ of *G. inflata* is lower compared to $\delta^{13}C_{DIC}$ and does not mirror the decreasing $\delta^{13}C_{DIC}$ values with depth. Our data indicate quite the reverse: the $\delta^{13}C$ of *G. inflata* slightly increases with depth in the water column.

Fig. 7a illustrates that no relation exists when $\delta^{13}C_{inflata}$ (250–355 μm) is plotted versus $\delta^{13}C_{DIC}$. Why is the $\delta^{13}C$ of *G. inflata* not reflecting the gradient seen in the $\delta^{13}C_{DIC}$ profile?

Laboratory culture experiments (Spero et al., 1997) revealed that the seawater $[CO_3^{2-}]$ affects the $\delta^{13}C$ of planktic foraminiferal calcite: an increase in the $[CO_3^{2-}]$ results in a decrease in the carbon isotope values in the shells of foraminiferal species. Our field data in the Cape Basin show a decrease of the $[CO_3^{2-}]$ from 250 $\mu mol \cdot kg^{-1}$ near the sea surface to 130 $\mu mol \cdot kg^{-1}$ at 500 m water depth (Table 3). This allows us to evaluate the carbonate ion effect on $\delta^{13}C$ of *G. inflata* during its depth integrated calcification process. As shown above, *G. inflata* secretes parts of its shell at different depths in the water column. Hence, a direct comparison of the measured $\delta^{13}C_{shell}$ data of *G. inflata* to the in situ $[CO_3^{2-}]$ found at the collection depth is incorrect. To correct the $\delta^{13}C_{shell}$ value at a given depth for the isotopic composition of the calcite that has been built at shallower levels in the water column, we calculated depth interval added $\delta^{13}C$ ($\delta^{13}C_{IA}$) composition for each plankton tow interval. Thus the $\delta^{13}C$ value of the additionally grown calcite within a given interval is calculated as (see Appendix for details):

$$\delta^{13}C_{IA} = \frac{m_i \cdot \delta^{13}C_{shell,i} - m_{i-1} \cdot \delta^{13}C_{shell,i-1}}{(m_i - m_{i-1})} \qquad (3)$$

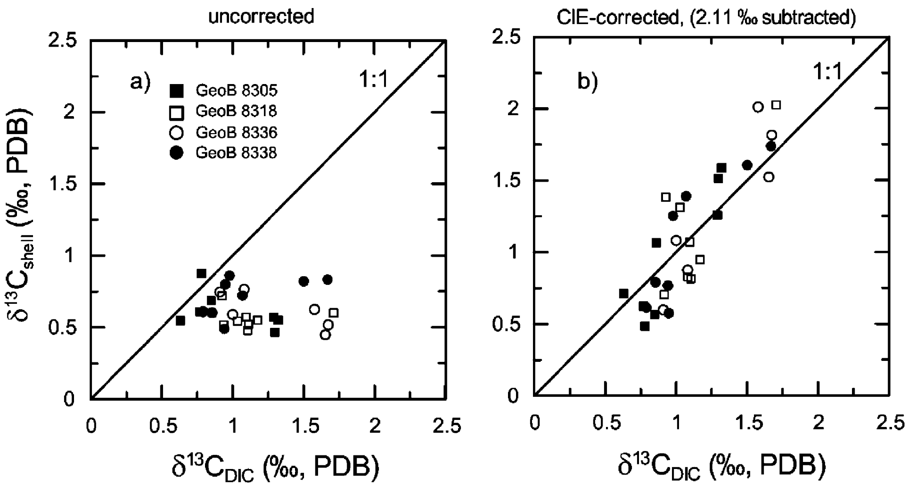

Fig. 7. (a) Uncorrected $\delta^{13}C_{DIC}$ versus $\delta^{13}C_{shell}$ values for *G. inflata* (250–355 μm) in the upper water column. The $\delta^{13}C$ values of *G. inflata* are nearly constant with varying $\delta^{13}C_{DIC}$. (b) Carbonate ion effect corrected $\delta^{13}C_{DIC}$ versus $\delta^{13}C_{shell}$ values for *G. inflata* (250–355 μm) in the upper water column. The $\delta^{13}C$ values of *G. inflata* respond to $\delta^{13}C_{DIC}$ variations, as expected from laboratory culture experiments. For the correction to a carbonate ion concentration of 0 μmol kg$^{-1}$, we used the slopes derived for *G. inflata* via weighted $\Delta\delta^{13}C_{IA\text{-}DIC}/[CO_3^{2-}]$ correlation. From the 1:1 slope the correlation shows an average offset of about 2.11.

For the upper most interval $\delta^{13}C_{shell,i}$ is equal to the measured $\delta^{13}C_{shell}$. We then subtract the $\delta^{13}C_{DIC}$ value from the $\delta^{13}C_{IA}$ for each interval, and plotted the obtained $\Delta\delta^{13}C_{IA\text{-}DIC}$ versus the $[CO_3^{2-}]$ that was obtained for this interval.

Fig. 8 shows that the $\Delta\delta^{13}C_{IA\text{-}DIC}$ correlates with $[CO_3^{2-}]$ at the four stations. We find slopes of $-0.013$‰ to $-0.015$‰ (μmol kg$^{-1}$)$^{-1}$ for the large size fractions (250–355 μm). The smaller specimens show similar slopes between $-0.013$‰ and $-0.017$‰ (μmol kg$^{-1}$)$^{-1}$. However, at station 8318, which is located on the shelf, the $\Delta\delta^{13}C_{IA\text{-}DIC}$ versus $[CO_3^{2-}]$ yields steeper slopes. Responsible for this is a data point at 250 m. If we exclude the value from the deepest net, the regression slope adjust to $-0.013$‰ (μmol kg$^{-1}$)$^{-1}$. This observation suggest that probably a different water mass was present below 200 m on the shelf, which would explain the shift of $\delta^{13}C_{DIC}$ to higher values at this station below 200 m.

Table 3
Carbonate system data: alkalinity, DIC, pH and $CO_3^{2-}$ at the four stations in the Cape Basin

| GeoB station | Depth (m) | Alkalinity (μmol kg$^{-1}$)[a] | DIC (μmol kg$^{-1}$)[b] | pH[c] | $CO_3^{2-}$ (μmol kg$^{-1}$)[d] |
|---|---|---|---|---|---|
| 8305 | 10 | 2374.25 | 2039.53 | 8.244 | 242.0 |
| | 30 | 2365.74 | 2029.29 | 8.248 | 242.7 |
| | 50 | 2388.35 | 2093.25 | 8.189 | 215.9 |
| | 90 | 2364.11 | 2122.23 | 8.200 | 176.8 |
| | 250 | 2342.92 | 2128.91 | 8.217 | 155.5 |
| | 400 | 2334.06 | 2149.27 | 8.190 | 135.2 |
| 8318 | 10 | 2362.36 | 2106.09 | 8.161 | 188.90 |
| | 50 | 2364.57 | 2139.55 | 8.159 | 166.5 |
| | 90 | 2340.63 | 2155.13 | 8.106 | 140.2 |
| | 150 | 2323.24 | 2120.36 | 8.169 | 150.47 |
| | 250 | 2323.96 | 2140.01 | 8.140 | 136.8 |
| 8336 | 10 | 2361.42 | 2043.00 | 8.227 | 231.0 |
| | 50 | 2361.38 | 2061.30 | 8.239 | 216.3 |
| | 150 | 2335.15 | 2090.43 | 8.204 | 177.6 |
| | 250 | 2334.59 | 2127.44 | 8.161 | 152.4 |
| | 400 | 2322.93 | 2168.48 | 8.068 | 135.2 |
| 8338 | 10 | 2348.52 | 2058.98 | 8.185 | 211.6 |
| | 50 | 2348.47 | 2082.23 | 8.129 | 194.0 |
| | 90 | 2329.02 | 2104.41 | 8.160 | 165.0 |
| | 400 | 2306.75 | 2157.18 | 8.100 | 113.9 |

[a]Titration; [b]measured with continuous flow technique; [c,d]calculated using CO2SYS.

Model results by Zeebe et al. (1999) suggest that the magnitude of the carbonate ion effect is species-specific. The $\delta^{13}C/[CO_3^{2-}]$ slope observed in laboratory experiments for other non-symbiotic species, such as *G. bulloides* ($-0.013$‰ (μmol kg$^{-1}$)$^{-1}$) was about twice the slope of symbiotic species *O. universa* ($-0.006$‰ (μmol kg$^{-1}$)$^{-1}$) or *Globigerinoides sacculifer* ($-0.005$‰ (μmol kg$^{-1}$)$^{-1}$) (Bijma et al., 1998). This implies that additional mechanisms such as an internal pool or kinetic isotope effects are active (Zeebe, 1999). Thus if we assume that in general the non-symbiotic species respond stronger to changes of the $[CO_3^{2-}]$ it is likely that the slope of *G. inflata* is similar to the slope of non-symbiotic *G. bulloides*, as evident from our measurements.

However, the $[CO_3^{2-}]$ is not the only factor that varies with depth in the water column. Because temperature and $[CO_3^{2-}]$ in seawater are correlated (Fig. 2) and show a similar vertical gradient within the water

Table 4
Stable oxygen and carbon isotopic composition of *G. inflata* in two size fractions (150–250 and 250–355 μm) from plankton samples and hydrographic data ($\delta^{13}C_{DIC}$, $\delta^{18}O_{eq}$ and temperature at stations GeoB8305, 8318, 8336 and 8338)

| GeoB station | Depth (m) | $\delta^{18}O$ (‰, PDB) | | $\delta^{13}C$ (‰, PDB) | | $\delta^{13}C_{DIC}$ (‰, PDB) | $\delta^{18}O_{eq}$ (‰, PDB) | Temp. (°C) |
|---|---|---|---|---|---|---|---|---|
| | | 150–250 μm | 250–355 μm | 150–250 μm | 250–355 μm | | | |
| 8305 | 0–20 | −0.74 | −0.70 | 0.26 | 0.55 | 1.32 | −0.670 | 21.1 |
| | 20–40 | −0.74 | −0.78 | 0.30 | 0.47 | 1.30 | −0.666 | 21.1 |
| | 40–60 | −0.71 | −0.55 | 0.15 | 0.57 | 1.29 | −0.502 | 20.2 |
| | 60–80 | −0.26 | −0.34 | 0.31 | 0.60 | 0.86 | 0.246 | 16.0 |
| | 80–100 | −0.10 | −0.33 | 0.24 | 0.55 | 0.63 | 0.754 | 13.2 |
| | 100–200 | 0.18 | 0.17 | 0.37 | 0.61 | 0.77 | 1.114 | 11.2 |
| | 200–300 | | 0.65 | | 0.69 | 0.85 | 1.440 | 9.2 |
| | 300–500 | | 1.03 | | 0.88 | 0.78 | 1.813 | 7.1 |
| 8318 | 0–20 | −0.36 | −0.41 | 0.21 | 0.60 | 1.71 | −0.166 | 17.9 |
| | 20–40 | | −0.36 | | 0.52 | 0.94 | 0.487 | 15.0 |
| | 40–60 | −0.30 | −0.14 | 0.27 | 0.54 | 1.04 | 0.699 | 13.8 |
| | 60–80 | −0.42 | −0.24 | 0.39 | 0.48 | 1.20 | 0.769 | |
| | 80–100 | 0.05 | −0.27 | 0.35 | 0.55 | 1.18 | 0.961 | 12.0 |
| | 100–150 | 0.38 | 0.20 | 0.44 | 0.52 | 1.12 | 1.122 | 11.9 |
| | 150–200 | 0.56 | 0.30 | 0.47 | 0.57 | 1.05 | 1.196 | 10.2 |
| | 200–300 | | 0.40 | | 0.72 | 0.93 | 1.268 | 10.2 |
| 8336 | 0–20 | | −0.70 | | 0.52 | 1.67 | −0.781 | 20.9 |
| | 20–40 | −0.63 | −0.52 | 0.38 | 0.63 | 1.58 | −0.658 | 20.8 |
| | 40–60 | −0.45 | −0.49 | 0.41 | 0.45 | 1.65 | 0.183 | 17.4 |
| | 60–80 | | | | | 1.10 | 0.486 | 15.3 |
| | 80–100 | | | | | 0.86 | 0.590 | 14.6 |
| | 100–200 | | −0.04 | | 0.59 | 1.00 | 0.754 | 13.4 |
| | 200–300 | | 0.51 | | 0.77 | 1.08 | 0.990 | 12.5 |
| | 300–500 | | 0.62 | | 0.75 | 0.91 | 1.410 | 11.0 |
| 8338 | 0–20 | −0.65 | −0.66 | 0.52 | 0.83 | 1.67 | −0.782 | 20.7 |
| | 20–40 | −0.70 | −0.43 | 0.69 | 0.82 | 1.50 | −0.375 | 19.0 |
| | 40–60 | −0.46 | −0.45 | 0.55 | 0.72 | 1.07 | 0.121 | 16.9 |
| | 60–80 | −0.43 | −0.37 | 0.53 | 0.86 | 0.98 | 0.539 | 14.6 |
| | 80–100 | −0.29 | −0.08 | 0.33 | 0.49 | 0.94 | 0.581 | 13.8 |
| | 100–200 | 0.02 | 0.32 | 0.30 | 0.60 | 0.86 | 0.733 | 12.3 |
| | 200–300 | 0.58 | 0.51 | 0.40 | 0.61 | 0.79 | 1.289 | 10.3 |
| | 300–500 | 0.57 | 0.66 | 0.32 | 0.80 | 1.01 | 1.505 | 7.7 |

column, one can expect that the changes in the $\Delta\delta^{13}C_{IA\text{-}DIC}$ also correlate well with temperature. No temperature dependent fractionation occurs during the process of inorganic calcite precipitation (Romanek et al., 1992), but temperature may have an influence on the foraminiferal metabolic rate (Bemis et al., 2000). These authors quantified the effect of metabolism on the $\delta^{13}C$ for *G. bulloides*. The carbon isotopic composition of *G. bulloides* shells decreases with increasing temperature ($-0.11‰\ °C^{-1}$), probably as a function of greater metabolic modification of $\delta^{13}C_{DIC}$ near the shell at higher temperatures. Although temperature may have an influence, we are not able here to separate both effects. However, the $\Delta\delta^{13}C_{IA\text{-}DIC}/[CO_3^{2-}]$ slopes from our field data are statistically identical to the slopes established from laboratory culture experiments, thus we suppose that the influence of temperature on the $\delta^{13}C_{IA\text{-}DIC}$ is negligible. We therefore conclude that the $\delta^{13}C$ of *G. inflata* is mainly controlled by the $\delta^{13}C_{DIC}$ of the seawater, and its $[CO_3^{2-}]$.

These results of this study may have significant implications for paleoceanographic studies. For example, Lea et al. (1999) calculated that an increased alkalinity during glacial times could account for nearly all of the observed reduced $\delta^{13}C$ values in planktic foraminifera. His conclusions offer an alternative explanation to the generally accepted explanation of changes in the terrestrial biosphere-to-ocean transfer of carbon that was put forward to explain the lower $\delta^{13}C_{DIC}$ of the glacial ocean (e.g. Shackleton, 1977).

Fig. 7b shows the correlation between the carbonate ion effect-corrected $\delta^{13}C$ of *G. inflata* and $[CO_3^{2-}]$ using the determined slopes. The offset from the 1:1 correlation averages 2.11‰. This suggests that $\delta^{13}C_{DIC}$ can be derived from $\delta^{13}C_{inflata}$ by correcting to a $[CO_3^{2-}]$ of 0 μmol $kg^{-1}$ and adding 2.11.

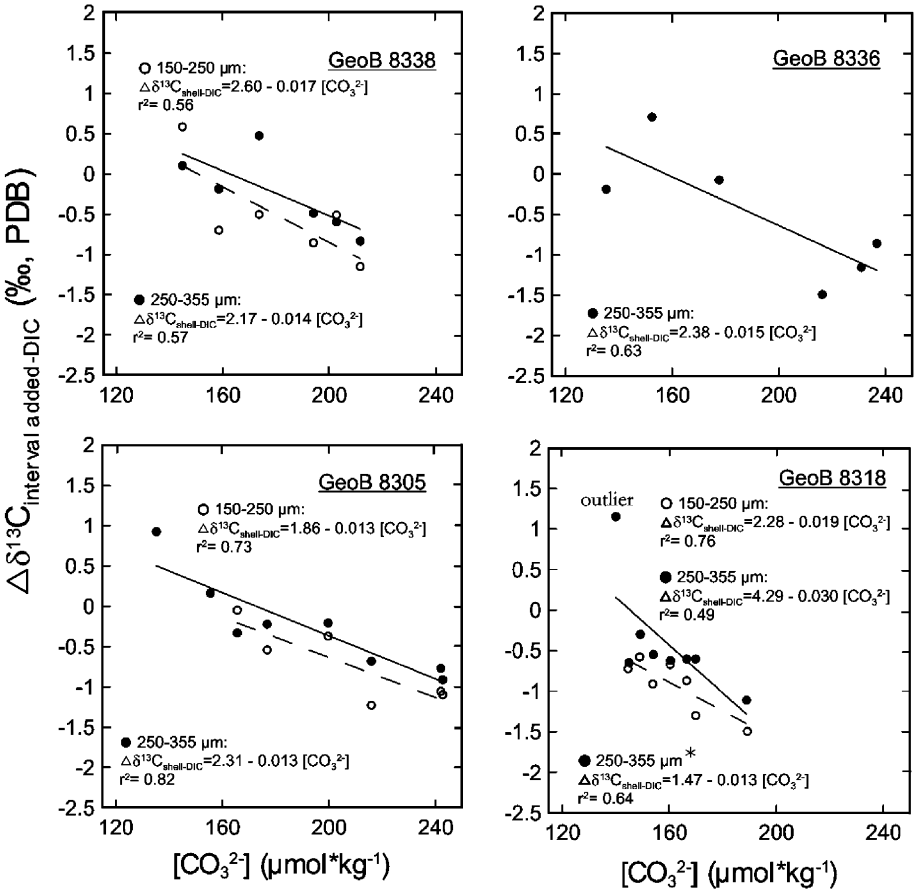

Fig. 8. $\delta^{13}C_{DIC}$ corrected $\delta^{13}C_{shell}$ values for *G. inflata* ($\Delta\delta^{13}C_{\text{IA-DIC}}$) versus the carbonate ion concentration ($[CO_3^{2-}]$) of the ambient seawater at stations GeoB8338, 8336, 8305 and 8318. Lines indicate linear regression: dashed line and open dots for the small size fraction, solid line and closed dots for the large size fraction. At station GeoB8318 (250–355 µm) the regression slope is steeper compared to the three other stations. If we exclude a data point from the deepest net (200–300 m), the slope adjusts to $-0.013$ (µmol kg$^{-1}$)$^{-1}$ (see 250–355 µm*).

### 5.4. Shell sizes

Another issue to be considered in the interpretation of the stable carbon isotope fractionation is the effect of changes in the metabolic activity during ontogeny. In general, the size of a planktic foraminifer increases with ontogeny, but also size variations due to temperature changes have been observed (Bijma et al., 1990; Spero and Lea, 1996).

In the upper most interval (0–20 m) of the water column we studied *G. inflata* in a wide range of shell sizes under constant hydrographic conditions (Fig. 9). As an example, the shell size of *G. inflata*, in the shallowest depth interval (0–20 m) at station GeoB8338, correlates positively with shell mass, i.e. larger individuals are indeed heavier in weight. At the same time the stable carbon isotope composition increases in general with shell size and shell mass, which was already shown for other species (e.g. Berger

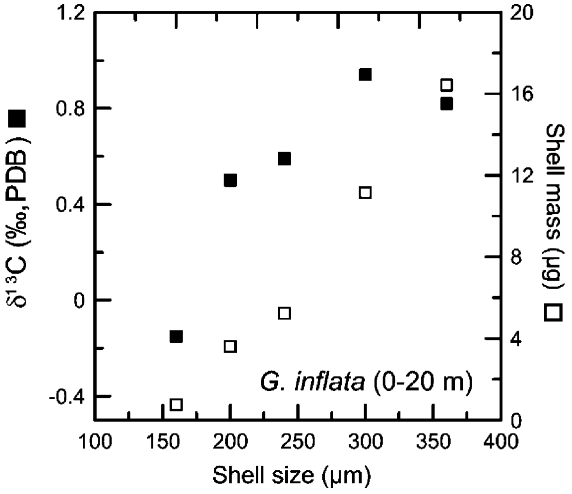

Fig. 9. Relationship between shell size (µm) and $\delta^{13}C$ (‰, PDB) and shell mass (µg) of *G. inflata* collected in the upper most depth interval (0–20 m). Both the $\delta^{13}C$ and the shell mass increase with increasing shell size.

et al., 1978; Spero and Lea, 1996; Bemis et al., 2000). Above ~300 μm the $\delta^{13}$C values remains almost constant, putting forward the question: What causes the differences in $\delta^{13}$C between different sizes?

The increase in $\delta^{13}$C-size trend may be attributed to ontogenetic/metabolic effect. In early ontogenetic life stages individuals may calcify faster respiring at higher rates (Berger et al., 1978; Hemleben et al., 1989). As a result higher amounts of respired $^{12}CO_2$ may be used during calcification in early life stages, explaining the lower $\delta^{13}$C of smaller specimens of *G. inflata* compared to larger ones.

## 6. Conclusion

We investigated the stable carbon and oxygen isotopes in calcite shells of planktic foraminifera species *G. inflata*, with special emphasis on the potential effect of the $[CO_3^{2-}]$ in seawater on the shell $\delta^{13}$C and $\delta^{18}$O.

While the increase of $\delta^{18}$O of *G. inflata* reflects the gradient observed in the predicted $\delta^{18}O_{eq}$ profile with depth in the water column, the $\delta^{13}$C of *G. inflata* does not mirror the $\delta^{13}C_{DIC}$ profile. We found no evidence for a relationship between the offsets from predicted $\delta^{18}O_{eq}$ and the $[CO_3^{2-}]$ of the ambient seawater for *G. inflata*.

Since the increase of the oxygen isotopic composition with depth indicates integrated shell growth of *G. inflata* that starts near the sea surface and continues down to 200–450 m depending on the hydrographic conditions, we used an oxygen isotope mass balance model to quantify the depth integrated growth of *G. inflata.* Based on this information, we are able to quantify the weighted $\Delta\delta^{13}C_{IA\text{-}DIC}$ changes as a function of the $[CO_3^{2-}]$. We find $\Delta\delta^{13}C_{IA\text{-}DIC}/[CO_3^{2-}]$ slopes for *G. inflata* which are similar to the ones established for other non-symbiotic species like *G. bulloides* from laboratory experiments. Hence, this suggests that the $\delta^{13}C_{DIC}$ and the carbonate chemistry of surface waters mainly control the carbon isotope composition of *G. inflata*. Our findings may bear important implications for paleoceanographic studies since large changes of the carbonate system between glacial and interglacial times are considered to have occurred.

In addition to the carbonate ion effect, the $\delta^{13}$C of *G. inflata* is influenced by a size-related ontogenetic/metabolic effect. Although found under same conditions (0–20 m) stable carbon isotope composition of *G. inflata* increases in general with shell size and shell mass, and shell size and shell mass are linearly correlated.

## Acknowledgments

We thank captains and crews of Meteor 57/1. We further thank M. Segl and B. Meyer-Schack for help with isotope analysis. Sylvia Kemle von Mücke helped in selecting and counting planktic foraminifera. Many thanks to Anja Terbrüggen from the Alfred-Wegener Institute in Bremerhaven who helped measure the total alkalinity titration and the DIC. D. Bauch and H. Spero are acknowledged for their constructive comments on an earlier version of the manuscript. This study was made possible through funding by the Deutsche Forschungsgemeinschaft (International Graduate College “Proxies in Earth History”, University Bremen) and by EU grant Nr.EVRI-2001-40018 (CESOP) to F.P.

## Appendix A. An oxygen isotope mass balance model to solve the problem of depth integrated shell growth

When studying the isotopic composition of field collected planktic foraminifera, the measured isotopic, or geochemical (e.g. Mg/Ca), composition of the test is often compared to ambient seawater properties to quantify the difference between measured and expected composition of the test or to perform field calibrations. Such calibrations, or comparisons, can only be made under the following assumptions: (1) It is assumed that the measured geochemical characteristic of the foraminifer test is indeed related to one (or potentially more) property of the ambient water. (2) It is assumed that the measured physical or chemical property or properties of the ambient seawater (e.g. temperature, nutrient concentration, $\delta^{18}O_w$, $\delta^{13}C_{DIC}$, etc.), that is relevant for the calibration, did not change substantially over the life span of the foraminifer considered. (3) It is assumed that the whole shell has grown at a more or less constant depth in the water column and, as such, has recorded the ambient seawater properties of the depth level at which all, or at least most, of its calcite was precipitated. For species that grow at relatively shallow depth levels, i.e. within the surface mixed layer of the upper water column, these assumptions seem quite reasonable. A problem, however, occurs when a given species migrate vertically, by descending to deeper water, during its life cycle. During vertical migration, a given specimen may have precipitated fractions of its total shell mass at different depth levels. Consequently, the chemical characteristics of its test cannot be related directly to the ambient seawater properties at one single depth level in the water column. In general, the physical and chemical properties of the upper ocean often change substantially with depth. Depending on the geographic location the temperature of seawater, for example, may easily drop by 10 or more degrees within the photic zone. Species of the genus *Globorotalia*, which are known to calcify down to a few hundreds of meters, thus have calcified parts of their shells under very different environmental conditions.

Our observations described in the manuscript allow us to estimate the fraction of shell mass that grows at different depth levels in the water column. In other words, the oxygen isotope composition may be used to calculate a mass balance assuming: (1) that shell growth (of all specimens) followed a unidirectional downward growth pattern, i.e. they started within the surface mixed layer and continue to add calcite with increasing depth, (2) the oxygen isotope composition of specimens caught at a given depth level is the result of the oxygen isotope composition of the previous depth level plus an additional amount of new calcite that is grown in equilibrium with the ambient seawater of the depth level under consideration. (3) Finally, it is assumed that the oxygen isotope composition of newly formed foraminiferal calcite within a given tow interval takes place in equilibrium with the ambient seawater composition within the interval considered. For $n$ plankton intervals, the expected oxygen isotope composition of a given specimen ($\delta^{18}\mathrm{O}^{*}_{\mathrm{shell},i}$) may be calculated as:

$$\delta^{18}\mathrm{C}^{*}_{\mathrm{shell},i} = \frac{\sum_{i-1}^{n}(m_i - m_{i-1})\cdot\delta^{18}\mathrm{O}_{\mathrm{eq},i}}{m_i}$$

In this equation $i$ represents the plankton "tow number", starting with 1 for the surface net and higher numbers for deeper nets. The average mass of foraminifera within each interval $i$ is given by $m_i$. Note that for $i=1$, the shallowest net, it is necessary to use $m_{i\text{-}1}=0$. Furthermore, $\delta^{18}\mathrm{O}_{\mathrm{eq},i}$ represents the interval averaged oxygen isotope composition of equilibrium calcite for tow interval $i$. In addition, it is easy to see that test growth between two successive tow intervals is equal to $m_i - m_{i\text{-}1}$. At a given depth level in the water column, it can be expected that shell growth ceases. The depth level in the water column at which shell growth ceases is referred to as the base of the productive zone. Below the productive zone, the $\delta^{18}\mathrm{O}_{\mathrm{shell}}$ remains approximately constant, because no calcite is added to the foraminiferal test.

The characteristic gradual increase of the oxygen isotope composition of specimens below the surface mixed layer including the "history effect" appears to be features we often observe in the oxygen isotope composition of plankton tow collected foraminifera (see Fig. 5). Our proposed method thus may be used to estimate quantitatively the relative amount of shell mass that is added to the shell with increasing depth. By using the oxygen isotope composition of specimens collected at different depth intervals in the upper water column, one will thus be able to quantify depth-integrated growth.

In this manuscript we use this oxygen isotope mass balance approach to unravel the relationship between the carbon isotope composition of *G. inflata* and the in situ $[\mathrm{CO}_3^{2-}]$ at different depth levels in the water column. For each plankton tow interval we calculate the fraction of calcite formed within this interval, which is then used to "correct" the shell value $\delta^{13}\mathrm{O}_{\mathrm{shell},i}$ for the "history effect". In formula, we can write for the carbon isotope composition of a given specimen within depth interval $i$:

$$\delta^{13}\mathrm{C}_{\mathrm{shell},i} = \frac{(m_i - m_{i-1})\cdot\delta^{13}\mathrm{C}_{\mathrm{IA}} + m_{i-1}\cdot\delta^{13}\mathrm{C}_{\mathrm{shell},i}}{m_i}$$

By rewriting this equation for the carbon isotope composition of the newly formed calcite within interval $i$, this yields:

$$\delta^{13}\mathrm{C}_{\mathrm{IA}} = \frac{m_i\cdot\delta^{13}\mathrm{C}_{\mathrm{shell},i} - m_{i-1}\cdot\delta^{13}\mathrm{C}_{\mathrm{shell},i}}{m_i - m_{i-1}}$$

For every depth interval at a given station, the carbon isotope composition of the newly formed calcite can now be plotted versus the in situ measure carbonate ion concentrations, in order to investigate its potential effect.

## References

Archer, D., Maier-Reimer, E., 1994. Effect of deep-sea sedimentary calcite preservation on atmospheric $\mathrm{CO}_2$ concentration. Nature 367, 260–263.

Bauch, D., Erlenkeuser, H., Winckler, C., Pavlova, G., Thiede, J., 2002. Carbon isotopes and habitat of polar planktic foraminifera in the Okhotsk Sea: the "carbonate ion effect" under natural conditions. Marine Micropaleontology 871, 1–17.

Bé, A.W.H., Hutson, W.H., 1977. Ecology of planktonic foraminifera and biogeographic patterns of life and fossil assemblages in the Indian Ocean. Micropaleontology 23, 369–414.

Bé, A.W.H., Hembleben, C., Anderson, O.R., Spindler, M., Hacunda, J., Tuntivate-Choy, S., 1977. Laboratory and field observations of living planktonic foraminifera. Micropaleontology 23, 155–179.

Bemis, B., Spero, H.J., Lea, D.W., Bijma, J., 2000. Temperature influence on the carbon isotopic composition of *Orbulina universa* and *Globigerina bulloides* (planktic foraminifera). Marine Micropaleontology 38, 213–228.

Berger, W.H., Killingley, J.S., Vincent, E., 1978. Stable isotopes in deep-sea carbonates: Box Core ERDS-92 west equatorial Pacific. Oceanologica Acta 1, 203–216.

Bijma, J., Faber, W.W., Hemleben, C., 1990. Temperature and salinity limits for growth and survival of some planktonic foraminifers in laboratory cultures. Journal of Foraminiferal Research 20, 95–116.

Bijma, J., Spero, H.J., Lea, D.W., 1998. Oceanic carbonate chemistry and foraminiferal isotopes: new laboratory results paper presented at the Sixth International Conference on Paleoceanography, Lisbon, 1998.

Bouvier-Soumagnac, Y., Duplessy, J.-C., 1985. Carbon and oxygen isotopic composition of planktonic foraminifera from laboratory culture, plankton tows and recent sediment: implication for the reconstruction of paleoclimatic conditions and of the global carbon cycle. Journal of Foraminiferal Research 15, 302–320.

Broecker, W.S., Maier-Reimer, E., 1992. The influence of air and sea exchange on the carbon isotope distribution in the sea. Global Biogeochemical Cycles 6, 315–320.

Broecker, W.S., Peng, T.-H., 1982. Tracers in the sea. Lamont-Doherty geological observatory, University of Columbia, Palisades, New York 10964. 690 pp.

Charles, C.D., Wright, J.D., Fairbanks, R.G., 1993. Thermodynamic influences on the marine carbon isotope record. Paleoceanography 8, 691–697.

Dickson, A.G., 1990. Thermodynamics of the dissociation of boric acid in synthetic seawater from 273.15 to 318.15 K. Deep Sea Research 37, 755–766.

Duplessy, J.-C., Labeyrie, L.D., Juillet-Leclerc, A., Maitre, F., Duprat, J., Sarnthein, M., 1991. Surface salinity reconstruction of the North Atlantic Ocean during the last glacial maximum. Oceanologica Acta 14 (4), 311–324.

Fairbanks, R.G., Sverdlove, M., Free, R., Wiebe, P.H., Be, A.W.H., 1982. Vertical distribution and isotopic fractionation of living planktonic foraminifera from the Panama Basin. Nature 298, 841–844.

Gordon, A.L., 1996. Comment on the South Atlantic's role in the global circulation. In: Wefer, G., Berger, W.H., Siedler, G., Webb, D.J. (Eds.), The South Atlantic: Present and past circulation. Springer Verlag, Berlin Heidelberg, pp. 121–124.

Hemleben, C., Spindler, M., Anderson, O.R., 1989. Modern Planktonic Foraminifera. Springer Verlag, New York. 363 pp.

Itou, M., Ono, T., Oba, T., Noriki, S., 2001. Isotopic composition and morphology of living *Globorotalia scitula*: a new peoxy of subintermediate ocean carbonate chemistry? Marine Micropaleontology 42, 189–210.

Jouzel, J., Barkov, N.I., Barnola, J.M., Bender, M., Chappellaz, J., Genthon, C., Kotlyakov, V.M., Lipenkov, V., Lorius, C., Petit, J.R., Raynaud, D., Raisbeck, G., Ritz, C., Sowers, T., Stievenard, M., Yiou, F., Yiou, P., 1993. Extending the Vostok ice-core record of palaeoclimate to the penultimate glacial period. Nature 364, 407–412.

Kahn, M.I., Williams, D.F., 1981. Oxygen and carbon isotopic composition of living planktonic foraminifera from the northeast Pacific Ocean. Palaeogeography, Palaeoclimatology, Palaeoecology 33, 47–69.

Kim, S.-T., O'Neil, J.R., 1997. Equilibrium and non-equilibrium oxygen isotope effects in synthetic carbonates. Geochimica et Cosmochimica Acta 61, 3461–3475.

King, A.L., Howard, W.R., 2005. $\delta^{18}$O seasonality of planktonic foraminifera from Southern Ocean sediment traps: latitudinal gradients and implications for paleoclimate reconstructions. Marine Micropaleontology 56, 1–24.

Kroon, D., Ganssen, G., 1989. Northern Indian Ocean upwelling cells and the stable isotope composition of living planktonic foraminifers. Deep Sea Research 36, 1219–1236.

Lea, D.W., Bijma, J., Spero, H.J., Archer, D., 1999. Implications of a carbonate ion effect on shell carbon and oxygen isotopes for glacial ocean conditions. In: Fischer, G., Wefer, G. (Eds.), Use of proxies in paleoceanography: Examples from the South Atlantic. Springer, Berlin, pp. 513–522.

Lewis, E., Wallace, D.W.R., 1998. Program Developed for $CO_2$ System Calculations. ORNL/CDIAC-105. Carbon Dioxide Information Analysis Center, Oak Ridge National Laboratory. U.S. Department of Energy, Oak Ridge, Tennessee.

Lynch-Stieglitz, J., Stocker, T.F., Broecker, W.S., Fairbanks, R.G., 1995. The influence of air–sea gas exchange on the isotopic composition of oceanic carbon: observations and modelling. Global Biogeochemical Cycles 9, 653–665.

Millero, F.J., 1979. The thermodynamics of the carbonate system in seawater. Geochimica et Cosmochimica Acta 43, 1651–1661.

Millero, F.J., 1995. Thermodynamics of the carbon dioxide system in the oceans. Geochimica et Cosmochimica Acta 59, 661–677.

Mulitza, S., Arz, H., Kemle-von Mücke, S., Moos, C., Niebler, H.S., Pätzold, J., Segl, M., 1999. The South Atlantic carbon isotope record of planktic foraminifera. In: Fischer, G., Wefer, G. (Eds.), Use of proxies in paleoceanography: Examples from the South Atlantic. Springer, Berlin, pp. 427–445.

Peeters, F.J.C., Brummer, G.J.A., 2002. The seasonal and vertical distribution of living planktic foraminifera in the NW Arabian Sea. In: Clift, P.D., Kroon, D., Gaedicke, C., Craig, J. (Eds.), The Tectonic and Climatic Evolution of the Arabian Sea Region. Geological Society, London, pp. 463–497.

Peeters, F.J.C., Brummer, G.-J., Ganssen, G., 2002. The effect of upwelling on the distribution and stable isotope composition of *Globigerina bulloides* and *Globigerinoides ruber* (planktic foraminifera) in modern surface waters of the NW Arabian Sea. Global and Planetary Change 34, 269–291.

Peeters, F.J.C., Acheson, R., Brummer, G.J.A., de Ruijter, W.P.M., Schneider, R., Ganssen, G., Ufkes, E., Kroon, D., 2004. Vigorous exchange between the Indian and Atlantic oceans at the end of the past five glacial periods. Nature, 661–665.

Petit, J.R., Jouzel, J., Raynaud, D., Barkov, N.I., Barnola, J.-M., Basile, I., Bender, M., Chappellaz, J., Davis, M., Delaygue, G., Delmotte, M., Kotlyakov, V.M., Legrad, M., Lipenkov, V.Y., Lorius, C., Pepin, L., Ritz, C., Saltzman, E., Stievenard, M., 1999. Climate and atmospheric history of the past 420,000 years from the Vostok ice core, Antarctica. Nature 399, 429–436.

Prell, W.L., Curry, W.B., 1981. Faunal and isotopic indices of monsoonal upwelling: Western Arabian Sea. Oceanol Acta 4, 333–351.

Ravelo, A.C., Fairbanks, R.G., 1995. Carbon isotopic fractionation in multiple species of planktonic foraminifera from core-tops in the tropical Atlantic. Journal of Foraminiferal Research 25, 53–74.

Romanek, C.S., Grossman, E.L., Morse, J.W., 1992. Carbon isotopic fractionation in synthetic aragonite and calcite: effects of temperature and precipitation rate. Geochimica et Cosmochimica Acta 56, 419–430.

Roy, R.N., Roy, L.N., Vogel, K.M., Porter-Moore, C., Pearson, T., Good, C.E., Millero, F.J., Campbell, D.M., 1993. The dissociation constants of carbonic acid in seawater at salinities 5 to 45 and temperatures 0 to 45 °C. Marine Chemistry 44, 249–267.

Russell, A.D., Spero, H.J., 2000. Field examination of the oceanic carbonate ion effect on stable isotopes in planktonic foraminifera. Paleoceanography 15, 43–52.

Sanyal, A., Hemming, N.G., Hanson, G.N., Broecker, W.S., 1995. Evidence for a higher pH in the glacial ocean from boron isotopes in foraminifera. Nature 373, 234–236.

Schneider, R. et al., 2003. Report and Preliminary Results of Meteor Cruise M57/1, Cape Town-Walvis Bay, 20.01.-08.02.2003. Berichte Fachbereich Geowissenschaften, Universität Bremen 90, 216, 123 pp.

Shackleton, N.J., 1977. $^{13}$C in Uvigerina: tropical rainforest history and the equatorial Pacific carbonate dissolution cycles. In: Anderson, N., Malahof, A. (Eds.), Fate of Fossil Fuel $CO_2$ in the Oceans. Plenum, New York, pp. 401–427.

Shackleton, N.J., Vincent, E., 1978. Oxygen and carbon isotope studies in recent foraminifera from the southwest Indian Ocean. Marine Micropaleontology 19, 275–285.

Shannon, L.V., 1985. The Benguela ecosystem: 1. Evolution of the Benguela, physical features and processes. In: Barnes, M. (Ed.), Oceanography and Marine Biology: An Annual Review. University Press, Aberdeen, pp. 1–85.

Shannon, L.V., Nelson, G., 1996. The Benguela: Large scale features and processes and system variability. In: Wefer, G., Berger, W.H., Siedler, G., Webb, D.J. (Eds.), The South Atlantic Past and Present Circulation. Springer, Berlin Heidelberg, pp. 163–210.

Spero, H.J., 1992. Do planktic foraminifera accurately record shifts in the carbon isotopic composition of seawater $\sum CO_2$? Marine Micropaleontology 19, 275–285.

Spero, H.J., Lea, D.W., 1996. Experimental determination of stable isotope variability in *Globigerina bulloides*: implications for paleoceanographic reconstruction. Marine Micropaleontology 28, 231–246.

Spero, H.J., Bijma, J., Lea, D.W., Bemis, B., 1997. Effect of seawater carbonate concentration on foraminiferal carbon and oxygen isotopes. Nature 390, 497–500.

Stoll, M.H.C., Bakker, K., Nobbe, G.H., Haese, R.R., 2001. Continuous flow analysis of dissolved inorganic carbon content in seawater. Analytical Chemistry 73, 4111–4116.

Thiede, J., 1975. Distribution of foraminifera in surface waters of a coastal upwelling area. Nature 253, 712–714.

Valentine, H.R., Lutjeharms, J.R.E., Brundrit, G.B., 1993. The water masses and volumetry of the southern Agulhas Current region. Deep-Sea Research: Part 1. Oceanographic Research Papers 40 (6), 1285–1305.

Wefer, G., Berger, W.H., 1991. Isotope paleontology: growth and composition of extant calcareous species. Marine Geology 100, 207–248.

Weiss, R.F., 1974. Carbon dioxide in water and seawater: the solubility of a non-ideal gas. Marine Chemistry 2, 203–215.

Zeebe, R.E., 1999. An explanation of the effect of seawater carbonate concentration on foraminiferal oxygen isotopes. Geochimica et Cosmochimica Acta 63, 2001–2007.

Zeebe, R.E., Bijma, J., Wolf-Gladrow, D.A., 1999. A diffusion-reaction model of carbon isotope fractionation in foraminifera. Marine Chemistry 64, 199–227.